

Cyclotron effective mass of a two-dimensional electron layer at the GaAs/Al_xGa_{1-x}As heterojunction subject to in-plane magnetic fields

L. Smrčka, P. Vašek, J. Koláček, T. Jungwirth, and M. Cukr

Institute of Physics, Academy of Science of the Czech Republic, Cukrovarnická 10, 162 00 Prague 6, Czech Republic

(Received 24 February 1995)

We have found that Fermi-surface contours of a two-dimensional electron gas at the GaAs/Al_xGa_{1-x}As interface deviate from the standard circular shape under the combined influence of an approximately triangular confining potential and the strong in-plane magnetic field. The distortion of a Fermi-surface contour manifests itself through an increase of the electron effective cyclotron mass which has been measured by the cyclotron resonance in the far-infrared transmission spectra and by the thermal damping of Shubnikov-de Haas oscillations in tilted magnetic fields with an in-plane component up to 5 T. The observed increase of the cyclotron effective mass reaches almost 5% of its zero field value which is in good agreement with results of a self-consistent calculation.

The electrons confined to the GaAs/Al_xGa_{1-x}As heterostructure form a quasi-two-dimensional electron gas. In a zero magnetic field, or if a magnetic field is applied perpendicularly to the confinement plane x - y , the electron motion can be separated into an electric contribution governed by the confining potential V_{conf} and a free in-plane motion which can be quantized into Landau levels. In this case, the electron gas can be considered as two dimensional and the component of the motion in the third dimension, perpendicular to the sample plane, can be neglected.

Subject to an in-plane magnetic field B_y , the electrons moving in the x direction are decelerated or accelerated by the combined effect of the crossed fields B_y and $E_z = -dV_{\text{conf}}(z)/dz$, depending on the form of the confining potential V_{conf} , while the electron motion in the y direction remains unmodified. The system no longer behaves as a strictly two-dimensional (2D) one and its third dimension must be taken into account. As pointed out already in Refs. 1 and 2, the subband separation, the 2D density of states, and the shape of the Fermi-surface contour become functions of the magnetic field B_y .

To probe the changes of the electron structure due to the in-plane magnetic field it is useful to add a perpendicular component B_z to B_y . When the perpendicular component is weak, the electron dynamic in the x - y plane can be described semiclassically. In the quasiclassical picture, the electrons move along real space trajectories with shapes similar to the shape of the Fermi contour, but multiplied by the scale factor $\hbar/|e|B_z$ and rotated by $\pi/2$. The "egglike" distortion of the Fermi-surface contour and, consequently, of the real space trajectory results in changes of the cyclotron motion of an electron which is characterized by the cyclotron frequency ω_c and the cyclotron effective mass m_c . It is well known that the quasiclassical cyclotron motion can be quantized using the standard Bohr-Sommerfeld rule which states that each real space trajectory encloses an integer number of flux quanta $\hbar/|e|$. Such a procedure yields a discrete spectrum of Landau levels and the density of states becomes a series of delta functions separated by $\hbar\omega_c$. The degeneracy

of each level is $2|e|B_z/h$, exactly as in the case of perpendicular magnetic fields.

The cyclotron effective mass m_c should not be confused with the electron effective mass which is, for the case of an "egglike" Fermi line corresponding to the approximately triangular well, a tensor and an anisotropic function of the position on the line. The cyclotron mass is related to the shape of the Fermi-surface contour by

$$m_c = \frac{\hbar^2}{2\pi} \oint \frac{dk}{|\nabla_k E|}, \quad (1)$$

where dk denotes an element of a length of the Fermi line. Moreover, in the case of two-dimensional systems a simple relation between the density of states g and the cyclotron mass of a single subband is obtained,

$$g = \frac{m_c}{\pi\hbar^2}. \quad (2)$$

Equations (1) and (2) have been known for a long time.^{3,4} Since then they were utilized many times. For an application to 2D systems, see, e.g., Ref. 5. Their detailed derivation and discussion for the case of combined parallel and perpendicular magnetic fields can be found in Ref. 6.

This work is devoted to both experimental and theoretical investigation of the cyclotron effective mass as a function of the in-plane component of the applied magnetic field. To determine m_c experimentally, we have measured the cyclotron resonance in the far-infrared transmission spectra and the thermal damping of the Shubnikov-de Haas (SdH) oscillations. The self-consistent calculation of the electronic structure and the cyclotron effective mass, based on the parameters of a molecular-beam-epitaxy (MBE) grown samples, was utilized to obtain the theoretical curves of $m_c(B_{||})$ dependence.

The samples employed are GaAs/Al_xGa_{1-x}As modulation doped heterojunctions prepared by MBE. On the top of (100) semi-insulating substrate we have grown first an AlAs/GaAs superlattice, followed by a 2- μm undoped GaAs buffer layer, an undoped 10-nm

GaAs/Al_{0.32}Ga_{0.68}As spacer layer, a 100-nm *n*-doped GaAs/Al_{0.32}Ga_{0.68}As layer ($1.7 \times 10^{18} \text{ cm}^{-3} \text{ Si}$), and finally a 20-nm GaAs cap layer. A part of a wafer was used to prepare a rectangular sample $8 \times 8 \text{ mm}^2$ for the cyclotron resonance experiments; the sample for the magnetoresistance measurements was shaped into Hall-bar geometry using a standard lithographic technique. Its length and width were $1100 \mu\text{m}$ and $100 \mu\text{m}$, respectively. The concentration of 2D electron gas at a heterojunction, $N_e = 5.2 \times 10^{11} \text{ cm}^{-2}$, and the mobility $\mu = 4.1 \times 10^5 \text{ cm}^2/\text{Vs}$, were determined from the Shubnikov–de Haas oscillations of the magnetoresistance and the resistivity, respectively, measured at a temperature of 4.2 K.

Experimental study of m_c dependence on the in-plane magnetic field started with the cyclotron resonance measurement. The employed laser based far-infrared spectrometer is described in detail elsewhere.⁷ The sample was placed in the 10-T superconducting solenoid, with the laser beam oriented in parallel with the coil axis and the magnetic field direction. A silicon bolometer served to record the radiation transmitted through the sample as a function of the sweeping magnetic field. Independent monitoring of the laser power by a pyroelectric detector, located outside the cryostat, enabled us to eliminate efficiently random fluctuations of the laser system. A calibrated Hall probe, located near the sample, was used to determine the magnetic field.

The cyclotron mass was calculated from the position of a transmission minimum on the magnetic field scale, according to the equation

$$m_c = \frac{|e|B_{\perp}\lambda}{2\pi c}, \quad (3)$$

where B_{\perp} denotes the perpendicular component of a magnetic field for which the resonance occurs, λ is the laser line wavelength, and c the light velocity.

In the standard configuration, the sample is oriented with the plane perpendicular to the magnetic field direction, i.e., there is no parallel field component. In that case, a laser line with $\lambda = 129.5 \mu\text{m}$ yields the effective mass $m_c = 0.0645$. To determine its field dependence, the sample was mounted at a tilt, to achieve approximately the same parallel and perpendicular components of the magnetic field. The angle between a normal to the sample plane and the field direction was found $43^{\circ}47'$ by an optical measurement. For a tilted sample three different laser lines were employed, with wavelengths $432.7 \mu\text{m}$, $163.0 \mu\text{m}$, and $133.1 \mu\text{m}$; their transmission curves are shown in Fig. 1. The corresponding resonance fields have nonzero parallel components and allow us to calculate the increase of the cyclotron mass with increasing in-plane magnetic field.

SdH oscillation damping was investigated in the superconducting magnet reaching the maximum field 7 T. The sample holder makes it possible to fix an arbitrary tilt of a sample with respect to the applied magnetic field direction. In our case, the perpendicular configuration and a configuration with the sample plane almost parallel with the magnetic field were employed. The Hall voltage, detected on the sample itself, was used as a measure

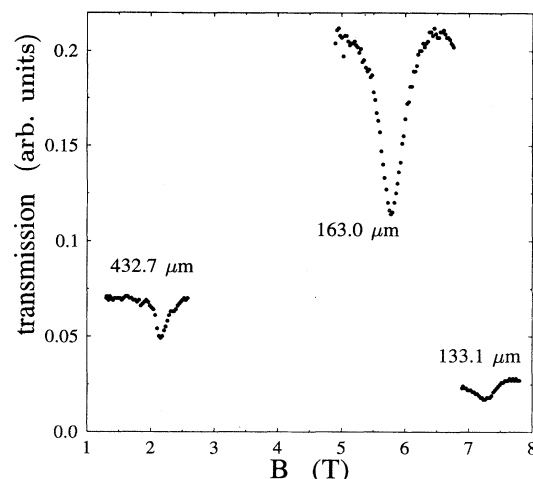


FIG. 1. Selected curves of the transmission coefficient of the infrared radiation through a tilted sample. The angle between the beam and the normal to the sample plane was $\alpha = 43^{\circ}47'$ and $T \approx 2 \text{ K}$.

of the perpendicular field component. The sample was immersed in the pumped ^4He bath and its temperature determined from the pressure of the gas.

The interpretation of experimental data is not so straightforward as in the case of cyclotron resonance. For the perpendicular magnetic field configuration, the detailed analysis of 2D electron gas subjected to low/intermediate fields⁸ showed that the oscillating part of the magnetoresistance is proportional to the oscillating part of the 2D density of states broadened by the zero field relaxation time τ . We assume that this type of behavior is preserved also in the case of tilted magnetic fields, only the quantities corresponding to $B_{\parallel} = 0$ should be replaced by that in $B_{\parallel} \neq 0$. Then we obtain an expression

$$\frac{\Delta\varrho}{\varrho_0} \propto \frac{\Delta g}{g} = 2 \sum_{s=1}^{\infty} \frac{X}{\sinh X} \exp\left(-\frac{\pi s}{\omega_c \tau}\right) \times \cos\left(\frac{2\pi^2 N_e s}{|e|B_{\perp}} - \pi s\right), \quad (4)$$

where the temperature damping factor X is given by

$$X = \frac{2\pi^2 k_B T m_c}{\hbar |e| B_{\perp}}. \quad (5)$$

Similarly as in the case of the cyclotron resonance, our study started with the sample subjected to perpendicular field. In that case the full Dingle plot can be used to find the effective mass m_c and the Dingle temperature $T_D = \hbar/2\pi k_B \tau$ with a high accuracy. The amplitudes of oscillations were determined from the magnetoresistance curves, after removing their smooth parts and higher harmonics by a digital filter.⁹ The value $m_c = 0.0658$ is in good agreement with $m_c = 0.0645$ obtained from the cyclotron resonance measurement and the widely accepted value $m_c = 0.067$. The Dingle temperature was equal to 1.31 K.

Since our equipment did not permit us to vary B_{\perp} and B_{\parallel} independently, the magnetoresistance $\Delta\rho/\rho$ was investigated in a tilted magnetic field with a fixed angle $80^{\circ}31'$ between the sample plane and the field direction. Figure 2 shows $\Delta\rho/\rho$ obtained with $j \parallel B_{\parallel}$ for several temperatures and plotted as a function of B . In this case each peak corresponds to a different B_{\parallel} and, therefore, $m_c(B_{\parallel})$ was determined from the temperature damping of individual peaks with a limited accuracy, similarly as in Ref. 10, where the SdH oscillations in a double-well structure were investigated. Again, the digital filter was applied to the data to gain curves comparable with the first, leading term of Eq. (4). It was also assumed that the relaxation time τ (the Dingle temperature T_D) does not depend on T and that, therefore, the exponential damping factor in (4) does not influence the temperature dependence of an amplitude at all.

Figure 3 presents the relative changes of the cyclotron effective mass obtained from both the cyclotron resonance measurement and the damping of SdH oscillation. The ratio $m_c(B_{\parallel})/m_c(0)$ is shown, instead of the raw data, to suppress possible systematic errors introduced into the results by uncertainties of magnetic field calibration and angle measurement in two experimental arrangements. The overall increase in m_c is approximately 5% in the maximum parallel field 5 T and there is quite acceptable agreement between the changes determined from the cyclotron resonance and SdH measurements. Together with the experimental data also the theoretical curves are shown.

Before discussing to what extent the theory agrees with the experimental data, we briefly describe the em-

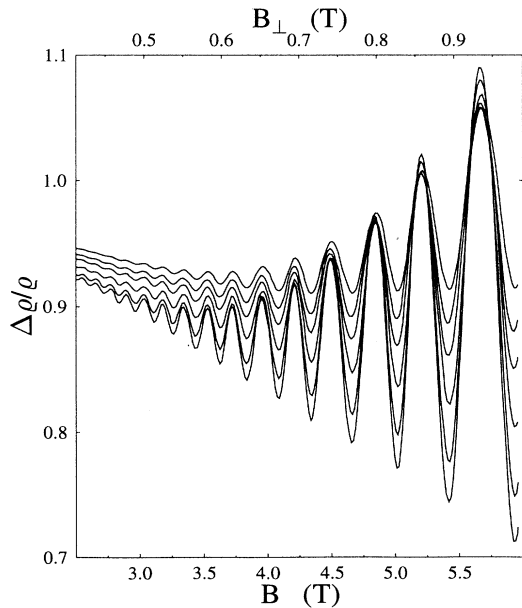


FIG. 2. Examples of magnetoresistance curves for a tilted sample, with the angle $\alpha = 9^{\circ}30'$, for the temperatures 2.70 K, 2.88 K, 3.15 K, 3.41 K, 3.59 K, and 3.82 K. Smooth parts of curves slightly increase with growing T , while the oscillation amplitudes are damped.

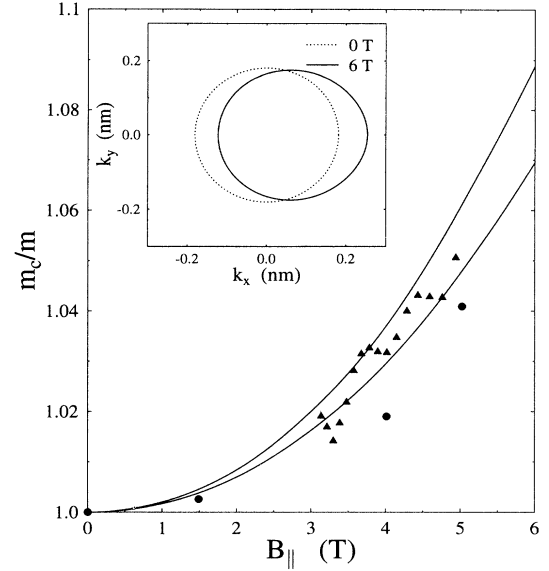


FIG. 3. Relative changes of the cyclotron effective mass m_c obtained from the cyclotron resonance measurement (circles) and the damping of SdH oscillation (triangles). The upper line is the theoretical curve calculated for the concentration of acceptors $N_a = 1.3 \times 10^{14} \text{ cm}^{-3}$, the second line for $N_a = 2.3 \times 10^{14} \text{ cm}^{-3}$. The inset demonstrates the variation of the Fermi line, corresponding to the lower concentration, caused by the applied in-plane magnetic field B_{\perp} .

ployed computational method. We have used a standard semiempirical model working quantitatively for the lowest conduction states of GaAs/As $_x$ Ga $_{1-x}$ As heterostructures. The coupled Poisson and Schrödinger equations are solved; the Schrödinger equation is treated in the envelope function approximation and envelope functions are assumed to be built from host quantum states belonging to a single parabolic band. Since the effect of the effective mass mismatch is completely neglected, the envelope functions of GaAs and Al $_x$ Ga $_{1-x}$ As are smoothly matched at the interface. The Hartree term of the confining potential is determined from the Poisson equation and we use the local density-functional approximation¹¹ of the exchange correlation term.

The input parameters for calculations were taken from our knowledge of samples described above. The conduction band offset V_b was determined from the AlAs fraction x according to a semiempirical rule

$$V_b = \alpha \times 1.247x \text{ (eV)}, \quad (6)$$

with the partition ratio α in the range 0.60–0.65,¹² the ionization energy of Si donors was taken as 60 meV. The concentration of donors was $N_d = 1.7 \times 10^{18} \text{ cm}^{-3}$. As for the acceptors, their energy levels are assumed to lie 1.514 eV below the conduction band bottom and the dielectric constant $\epsilon = 12.9$ was employed.

Similarly as in Ref. 13, we have found in the course of calculations that the results are relatively insensitive to

the exact values of most of these parameters, except for the concentration of residual acceptors in GaAs. Unfortunately, this quantity is difficult to measure and there is almost no information available concerning the homogeneity of their distribution in the z direction. Here we accepted the usual approximation of constant ionized impurities concentration $N_a^-(z) = N_a$ for $0 \leq z \leq l_a$, with the parameter l_a determined from the conditions of charge neutrality and the thermodynamical equilibrium in each loop of the self-consistent procedure. A series of different N_a has been tested. For presentation in Fig. 3, we have chosen two different "realistic" values corresponding to the standard level of impurities in our MBE samples, $N_a = 1.3 \times 10^{14} \text{ cm}^{-3}$ and $N_a = 2.3 \times 10^{14} \text{ cm}^{-3}$, and slightly modified α in Eq. (6), in the given range, to preserve the concentration N_e of free electrons

equal to the experimentally determined value $5.2 \times 10^{11} \text{ cm}^{-2}$.

Having in mind the above note about a semiempirical nature of the self-consistent calculations, we can conclude that there is a good agreement between the theoretically predicted field dependence of the cyclotron effective mass and the experimental data. We believe that the above described experimental methods might be appropriate for investigating the rich variety of Fermi-surface contours in quantum wells with diverse shapes of confining potential and in wider range of in-plane magnetic fields.

This work has been supported by the Academy of Science of the Czech Republic under Contracts No. 110 423 and No. 110 414, and by NSF, U.S., through Grant No. NSF INT-9106888.

¹ J. H. Crasemann, U. Merkt, and J. P. Kotthaus, Phys. Rev. B **28**, 2271 (1983).

² W. Zawadzki, S. Klahn, and U. Merkt, Phys. Rev. B **33**, 6916 (1986).

³ L. Onsager, Philos. Mag. **43**, 1006 (1952).

⁴ I. M. Lifshitz, M. J. Azbel, and M. I. Kaganov, Zh. Eksp. Teor. Fiz. **31**, 63 (1956) [Sov. Phys. JETP **30**, 63 (1956)].

⁵ T. G. Matheson and R. J. Higgins, Phys. Rev. B **25**, 2633 (1982).

⁶ L. Smrčka and T. Jungwirth, J. Phys. Condens. Matter **6**, 55 (1994).

⁷ J. Koláček, Z. Šimša, and R. Tesař, Meas. Sci. Technol. **4**, 1085 (1993).

⁸ A. Isihara and L. Smrčka, J. Phys. C **19**, 6777 (1986).

⁹ J. F. Kaiser and W. A. Reed, Rev. Sci. Instrum. **19**, 1103 (1978).

¹⁰ N. E. Harff, J. A. Simmons, S. K. Lyo, J. F. Klem, and S. M. Goodnick, in *22nd International Conference on Physics of Semiconductors, Vancouver*, edited by D. J. Lockwood (World Scientific, Singapore, 1994), p. 831; S. K. Lyo (unpublished).

¹¹ P. Ruden and G. H. Döhler, Phys. Rev. B **27**, 3538 (1983).

¹² S. Hiyamizu, in *Very High Speed Integrated Circuits: Heterostructure*, edited by T. Ikoma, Semiconductors and Semimetals Vol. 30 (Academic, Boston, 1990), p. 75.

¹³ F. Stern and S. Das Sarma, Phys. Rev. B **30**, 840 (1984).